PHYSICS AND CHEMISTRY OF SOLID STATE
V. 21, No. 4 (2020) pp. 689-694

Vasyl Stefanyk Precarpathian National University

ФІЗИКА І ХІМІЯ ТВЕРДОГО ТІЛА
Т. 21, № 4 (2020) С. 689-694

DOI: 10.15330/pcss.21.4.689-694

UDC 537.311.322 ISSN 1729-4428

V.A. Romaka[1], Yu. Stadnyk[2], L. Romaka[2], V. Krayovskyy[1],
A. Horyn[2], P. Klyzub[2], V. Pashkevych[1]

Study of the Structural, Electrokinetic and Magnetic Characteristics of the $Er_{1-x}Zr_xNiSb$ Semiconductor

[1]*National University "Lvivska Politechnika", Lviv, Ukraine, volodymyr.romaka@gmail.com*
[2]*Ivan Franko National University of Lviv, Lviv, Ukraine, lyubov.romaka@gmail.com*

Peculiarities of the structural, electrokinetic, energetic, and magnetic characteristics of $Er_{1-x}Zr_xNiSb$ semiconductive solid solution, x = 0 - 0.10, were studied. It was suggested that when Zr ($4d^25s^2$) atoms were introduced into the structure of the ErNiSb half-Heusler phase by substitution of Er ($5d^06s^2$) atoms in 4*a* position, Zr atoms can also simultaneously occupy the 4c position of Ni ($3d^84s^2$) atoms. As a result, in $Er_{1-x}Zr_xNiSb$ semiconductor, the structural defects of donor nature in position 4*a* and ones of acceptor nature in position 4*c* were generated simultaneously. In this case, in the band gap of $Er_{1-x}Zr_xNiSb$, the energy states of impurity donor ε_D^2 and acceptor ε_A^1 bands (donor-acceptor pairs) appear and determine the electrical conductivity mechanism of the semiconductor.

Keywords: electrical conductivity, thermopower coefficient, Fermi level.

Received 30 September 2020; Accepted 15 December 2020.

Introduction

RNiSb compounds and corresponding solid solutions (R – rare earth metal) are promising, but not enough studied class of thermosensitive materials with MgAgAs structure type. Study of the phase equilibria in the R–Ni–Sb ternary systems results in the existence of the equiatomic compounds [1]. However, for cases of light rare earth metals (La, Ce, Pr, Nd, Sm), the compounds crystallize in two structure types - AlB_2 and ZrBeSi [2, 3]. Instead, the RNiSb compounds with heavy rare earth crystallize in MgAgAs structure type. In turn, the antimonide GdNiSb exists in two structural modifications – high-temperature with hexagonal structure (AlB_2-type) and low-temperature one with MgAgAs-type. We will remind that Gd is in the middle of the lanthanide series and its 4*f*-shell contains 7 electrons out of 14.

RNiSb compounds, which have a structure of the MgAgAs type, are semiconductors and promising thermosensitive materials [4, 5]. This is the main motivator of our attention to this series of compounds. The combination of high thermoelectric characteristics and magnetic properties of half-Heusler phases based on rare earth and transition metals is a good starting point for a new class of thermoelectric materials.

In Refs. [6, 7] it was shown that the thermoelectric properties of half-Heusler phases in many cases strongly depend on heat treatment, which affects the defectivity of the crystal material. In this context, the study of phase equilibria in the corresponding system is an important step in understanding the influence of the preparation method, heat treatment, and charge and size factors on the existence of compounds and solid solutions based on them. Such studies will allow the synthesis of multicomponent thermosensitive materials with stable and reproducible characteristics up to the temperature of homogenizing annealing by doping the half-Heusler phases.

The study of the features of structural peculiarity, energetic and electrokinetic characteristics of the *p*-GdNiSb and *p*-LuNiSb semiconductors in the temperature range 4.2 - 400 K allowed to propose (offer) the model of the crystal structure for the LuNiSb compound [8]. Calculations of the density distribution of

electronic states (DOS) for *p*-LuNiSb showed that in the optimal variant of filling of crystallographic sites in the LuNiSb compound the band gap between energy levels of the valence band and conduction band appears, and the Fermi level ε_F is located near the edge of the valence band, which in the experiment correspond to positive values of the thermopower coefficient. This result completely corresponds to the experimental data.

At the optimal variant of the occupancy of crystallographic positions for the LuNiSb compound, the DOS calculations give the depth of occurrence of the Fermi level relative to the edge of the valence band ε_F= 23.9 meV, while from the electrokinetic measurements the value ε_F= 23.9 meV was obtained. Note that the accuracy of the calculations is ± 7 meV (width of the energy circuit (eV) to the number of points in the energy circuit). Taking into account the values of activation energy ε_1^{ρ} from the Fermi level ε_F to the percolation level of the valence band for *p*-LuNiSb determined from the high-temperature part of ln(ρ(1/*T*)) dependence, we sought the compensation degree of the semiconductor which will provide exactly such location of the Fermi level ε_F by DOS calculations. It was found the most acceptable and optimal variant of the atom distribution which provides the following occupancy of the crystallographic positions for LuNiSb compound: Ni(4*c*) = 92.65 % Ni + 1.35 % Lu + 6 % Vac; Lu(4*a*) = 100 % Lu; Sb(4*b*) = 100 % Sb. For other models of the atomic distribution, the band gap disappears, which assumes metallic conduction and does not agree with the results of electrokinetic studies [8].

In this context, the results of studies of thermosensitive materials based on half-Heusler phases, in particular the semiconductive $Er_{1-x}Zr_xNiSb$ solid solution, x = 0 - 0.15, in which the rare earth metal Er atoms have a local magnetic moment, seem to be interesting. In the present work the experimental results of the structural, electrokinetic, energetic and magnetic characteristics of the semiconductive $Er_{1-x}Zr_xNiSb$ solid solution, x = 0 - 0.15, are given. Our next paper will be devoted to a detailed study of the peculiarities of crystal and electronic structures of the ErNiSb compound, as well as the processes of their transformation with the introduction of impurity Zr atoms (the mechanism of generation of the structural defects and corresponding energetic levels).

I. Experimental details

The samples $Er_{1-x}Zr_xNiSb$, x = 0 - 0.15, were synthesized by arc melting of the initial components in an electric arc furnace under inert atmosphere of purified argon, followed by homogenizing annealing at 1073 K for 720 hours. To compensate for evaporation losses, 1 - 3 wt.% excess of Sb was added. Powder diffraction data were obtained on a powder diffractometer DRON-4.0 (Fe$K\alpha$-radiation). Crystallographic parameters were calculated using the program FullProf Suite [9]. The chemical and phase composition of the prepared alloys was examined by the method of electron probe microanalysis (EPMA) in combination with a scanning electron microscope-microanalyzer Tescan Vega 3 LMU (*K*- and *L*-spectral lines were used). The temperature and concentration dependencies of electrical resistivity and thermopower coefficient with pure copper as a reference material were measured in the temperature range 80-400 K. Magnetic susceptibility was measured by the Faraday method at 300 K.

II. Structural study of $Er_{1-x}Zr_xNiSb$

For the investigation, two series of the samples of the $Er_{1-x}Zr_xNiSb$ solid solution with a certain time interval were synthesized. X-ray structural studies of the $Er_{1-x}Zr_xNiSb$ solid solution showed that powder diffraction patterns of the two series samples were indexed with MgAgAs-type [4] and there were no reflections of the impurity phases. In turn, the study of the elemental composition of the surface of the samples established their correspondence to the composition of the charge.

A priori we reasoned as follows. If in the ErNiSb compound the Er atoms (r_{Er} = 0.178 nm) in position 4*a* is substituted by Zr atoms (r_{Zr} = 0.160 nm), it was expected that the lattice parameter values $a(x)$ would decrease, because the atomic radius Er is larger than Zr. However, the a(x) values of $Er_{1-x}Zr_xNiSb$ at concentrations x = 0 - 0.02 increase rapidly (Fig. 1). At higher concentrations, in the range x = 0.02 - 0.03, the $a(x)$ values decrease rapidly, and then similarly enlarge at x = 0.03 - 0.05. And only at x>0.05 lattice parameter values $a(x)$ of the $Er_{1-x}Zr_xNiSb$ thermosensitive material decrease.

Initially, we associated the nonmonotonic variation of the lattice parameter values $a(x)$ of $Er_{1-x}Zr_xNiSb$ with uncontrolled processes during sample preparation. After all, the accuracy of the X-ray diffraction method lies outside the concentrations of impurities in the semiconductor and does not allow them to be identified. However, the results of previous studies of the structural characteristics of $Er_{1-x}Zr_xNiSb$, in particular, changes in the lattice parameter values $a(x)$ for both series of

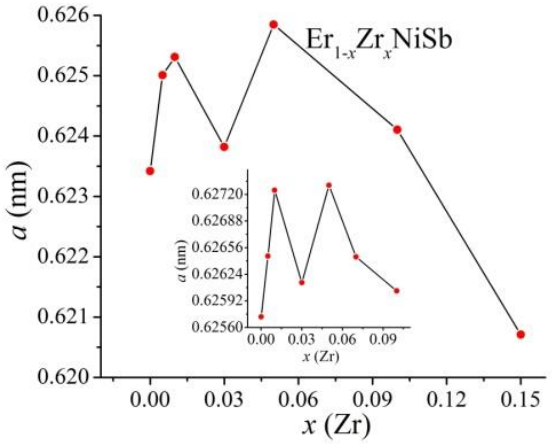

Fig. 1. Variation of the lattice parameter values $a(x)$ of $Er_{1-x}Zr_xNiSb$. Insert: variation of $a(x)$ for the samples prepared earlier.

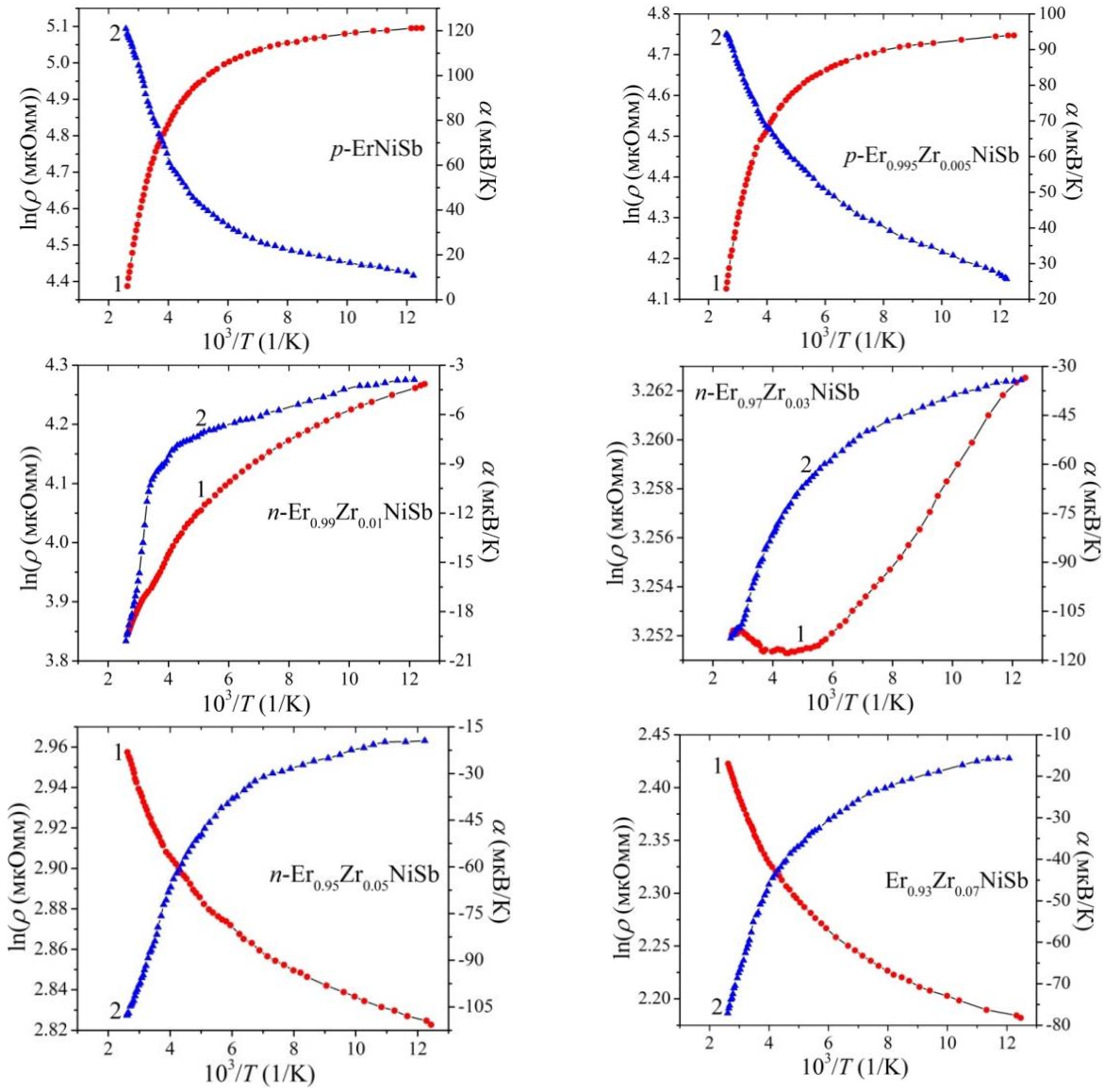

Fig. 2. Temperature dependencies of electrical resistivity ln($\rho(1/T)$) (1) and thermopower coefficient $\alpha(1/T)$ (2) for $Er_{1-x}Zr_xNiSb$

samples showed their similarity (Fig. 1). This suggests that the peculiarities detected in the $a(x)$ dependences of $Er_{1-x}Zr_xNiSb$ are a manifestation of changes in the structure during the introduction of Zr atoms and cannot be related to the quality of sample preparation by arc-melting the charge in an electric arc furnace followed by homogenizing annealing.

Thus, the behavior of the lattice parameter $a(x)$ of $Er_{1-x}Zr_xNiSb$ suggests that impurity Zr atoms introduced into half-Heusler ErNiSb phase may also partially occupy other crystallographic positions, in particular, 4c position of Ni atoms, or cause the appearance of other structural defects, for example, vacancies or atoms in the structural voids [6-8].

Considering, that the atomic radius of Ni (r_{Ni} = 0.124 nm) is the smallest in $Er_{1-x}Zr_xNiSb$ (r_{Sb} = 0.159 nm), the increase of the cell parameter $a(x)$ of the thermosensitive material $Er_{1-x}Zr_xNiSb$ can be caused only by the simultaneous partial occupation of 4*c* position of Ni atoms by impurity Zr atoms. By analogy, the increase of $a(x)$ values at x = 0.03 - 0.05 can also be explained by the displacement of Ni atoms from position 4c by Zr atoms. On the other hand, the substitution of Ni ($3d^84s^2$) atoms by Zr ($4d^25s^2$) atoms generates the structural defects of the acceptor nature in the crystal, because the Zr atom contains fewer *d*-electrons. In this case, the samples $Er_{1-x}Zr_xNiSb$, x = 0 - 0.02, will be semiconductors of the *p*-type conduction with positive values of the thermopower coefficient $\alpha(x,T)$.

The decrease of lattice parameter values $a(x)$ in the concentration range x = 0.02 - 0.03 can be caused by the occupation of 4*a* position of Er atoms ($4f^{12}6s^2$) by impurity Zr atoms, which generates the structural defects of donor nature. In the experiment, the thermopower coefficient values $\alpha(x,T)$ should be negative. The logic of reasoning is similar for samples of thermosensitive material $Er_{1-x}Zr_xNiSb$, $x > 0.05$, when lattice parameter $a(x)$ also decreases.

We are aware that the given above considerations concerning the elemental substitutions in the

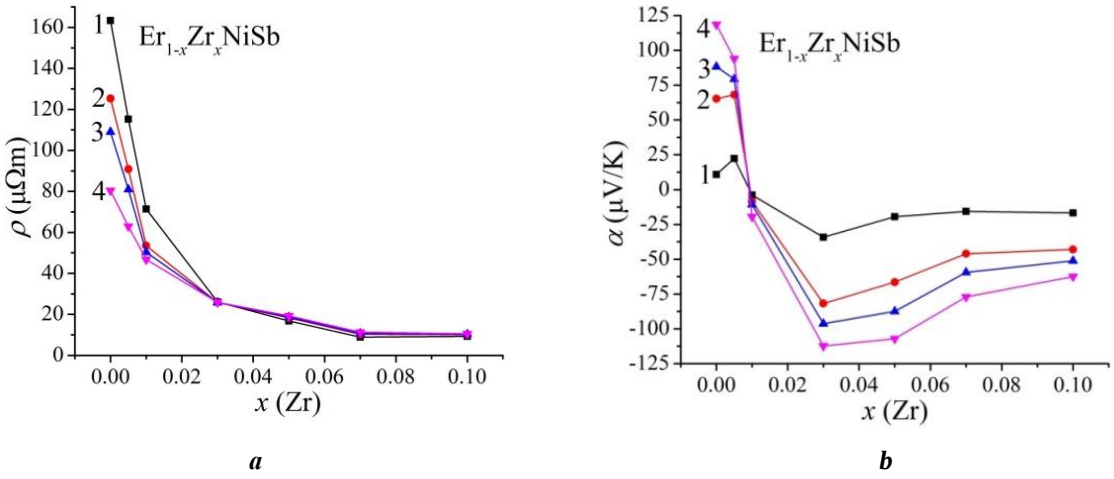

Fig. 3. Variation of the electrical resistivity values $\rho(x,T)$ (***a***) and thermopower coefficient $\alpha(x,T)$ (***b***) of $Er_{1-x}Zr_xNiSb$ at different temperatures: 1 – T = 80 K, 2 – T = 250 K, 3 – T = 300 K, 4 – T = 380 K.

$Er_{1-x}Zr_xNiSb$ structure are far from complex structural changes in the real crystal. Considering also the defective structure of the isostructural LuNiSb compound [8], in which vacancies (6 %) and Lu atoms (1.35 %) are available in the 4*c* position of Ni atoms, we can assume the complex character of changes in different crystallographic sites of $Er_{1-x}Zr_xNiSb$ solid solution.

The results of the study of the electrokinetic, energetic, and magnetic characteristics of $Er_{1-x}Zr_xNiSb$ samples, x = 0 - 0.15, combined with modeling of these characteristics allow to reduce in the future the variability of models of their crystal and electronic structures and establish a crystal structure as close as possible to the real state of the material.

III. Study of the electrokinetic, energetic and magnetic characteristics of $Er_{1-x}Zr_xNiSb$

Temperature and concentration dependencies of electrical resistivity ρ and thermopower coefficient α of the $Er_{1-x}Zr_xNiSb$ samples, x = 0 - 0.10, are shown in Figs. 2 and 3, respectively. The dependencies $\ln(\rho(1/T))$ and $\alpha(1/T)$ for $Er_{1-x}Zr_xNiSb$, x = 0 - 0.03, are typical for compensated semiconductors with activation regions and a change in the sign of thermopower coefficient $\alpha(T,x)$, which indicates the presence of several types of activation mechanisms of electrical conduction involving electrons and holes.

For samples $Er_{1-x}Zr_xNiSb$, $0 \le x \le 0.03$, in which the dependencies $\ln(\rho(1/T))$ have high-temperature activation parts, the Fermi level $\varepsilon_F$is located in the band gap. From the high-temperature activation parts of the $\ln(\rho(1/T))$ dependencies, the activation energy values ε_1^ρ from the Fermi level ε_F to the continuous energy bands are calculated, and from the $\alpha(1/T)$ dependencies the activation energy values ε_1^α, which give the values of the modulation amplitude of continuous energy bands of heavily doped and highly compensated semiconductor, are obtained [10].

In the case of the ErNiSb compound, the sign of the thermopower coefficient $\alpha(T,x)$ is positive and indicates the hole type of conduction, and the Fermi level is located near the valence band at a distance ε_1^ρ = 45.2 meV from the percolation level (Fig. 4). A similar location of the Fermi level ε_F was observed for RNiSb compounds (R = Gd, Lu) [8]. In turn, the modulation amplitude of continuous energy bands in the ErNiSb semiconductor is ε_1^α = 34.3 meV.

Assuming that in the ErNiSb compound, as in the case of LuNiSb, the crystallographic site 4*c* of Ni atoms is partially, up to ~ 1 %, occupied by Er atoms and characterized by vacancies (~ 6 %), then the structural defects of acceptor nature are generated in the crystal. This will lead to the appearance of several acceptor levels with different depth of occurrence in the band gap of the semiconductor, and the Fermi level ε_F is located near the percolation level of the valence band. In the experiment, the thermopower coefficient $\alpha(T, x)$ will have positive values. The suggested model of the atom arrangement in ErNiSb is in an agreement with the results of the electrokinetic studies (Figs. 2, 3).

We planned that the substitution of Er atoms by Zr

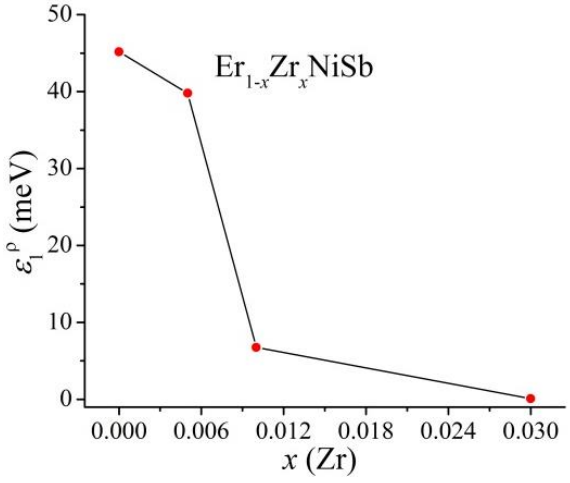

Fig. 4. Variation of the activation energy values $\varepsilon_1^\rho(x)$ of $Er_{1-x}Zr_xNiSb$.

ones in 4*a* position would generate donors in the crystal. In this case, the electrical resistivity values $\rho(x,T)$ should increase due to the reduction of the concentration of free holes during ionization of acceptors, and thermopower coefficient $\alpha(T,x)$ should change the sign from positive to negative. However, the introduction of the lowest in the experiment concentration of Zr atoms (x=0.005) into the structure of the ErNiSb compound did not change the sign of the thermopower coefficient $\alpha(T,x)$ and led to a decrease in the resistivity values $\rho(x,T)$ (Fig. 3). The depth of occurrence of the Fermi level ε_F relative to the percolation level of the valence band decreased to ε_1^{ρ} = 39.8 meV (Fig. 4).

The obtained result is unexpected, because for a *p*-type semiconductor this is possible only if the concentration of acceptor impurities increases, accompanied by an increase in the concentration of free holes, a drift of the Fermi level ε_F to the valence band, and a decrease of the electrical resistivity values $\rho(x,T)$ of $Er_{1-x}Zr_xNiSb$ at x = 0.005. Moreover, it turns out that the impurity Zr atoms do not generate donors and do not occupy crystallographic site 4*a* of Er atoms.

This experimental result shows that in the crystal structure of the $Er_{1-x}Zr_xNiSb$ semiconductor, x = 0.005, the changes take place, which generate the structural defects of acceptor nature and additional impurity acceptor level in the band gap. This is also indicated by the decrease of the modulation amplitude of the continuous energy bands of $Er_{1-x}Zr_xNiSb$ at x = 0.005 to value ε_1^{α} = 17.5 meV (Fig. 5, curve 1). This is possible in the case of occupation of the crystallographic position 4*c* of Ni atoms ($3d^84s^2$) by impurity Zr atoms, which generates the structural defects of acceptor nature in the crystal (Zr atom has fewer *d*-electrons than Ni).

The sign of thermopower coefficient $\alpha(T,x)$ of $Er_{1-x}Zr_xNiSb$ semiconductor, x = 0.01, becomes negative at all temperatures, and electrons are the main current carriers. At concentration x = 0.01, the Fermi level ε_F is located near the conduction band at a distance 6.7 meV from its percolation level. At higher concentrations of impurity Zr atoms ($0.01 < x$) the sign of the thermopower coefficient remains negative at all temperatures, the activation parts of $\ln(\rho(1/T))$ dependencies disappear, and the electrical resistivity values increase with temperature.

The metallization of electrical conductivity of $Er_{1-x}Zr_xNiSb$, $0.01 < x$, is a result of the movement of Fermi level ε_F to the conduction band of the semiconductor followed by crossing the percolation level of this band. Such behavior of the Fermi level ε_F is due to an increase in the concentration of donors, the ionization of which enlarges the number of free electrons. This result can be explained by the substitution of Er atoms in 4*a* position by Zr atoms, which will generate donors. In this case, the decrease of compensation degree takes place, as indicated by the decrease of the modulation amplitude of the continuous energy bands from ε_1^{α} = 11.7 meV at x = 0.01 to ε_1^{α} = 8.2 meV at x = 0.05 (Fig. 5).

Measurements of the magnetic susceptibility $\chi(x)$ of $Er_{1-x}Zr_xNiSb$ at T = 300 K (Fig. 5, curve 2) also point to the simultaneous generation of the defects of acceptor and donor nature in the crystal. The $Er_{1-x}Zr_xNiSb$ samples are Pauli paramagnets, the magnetic susceptibility of

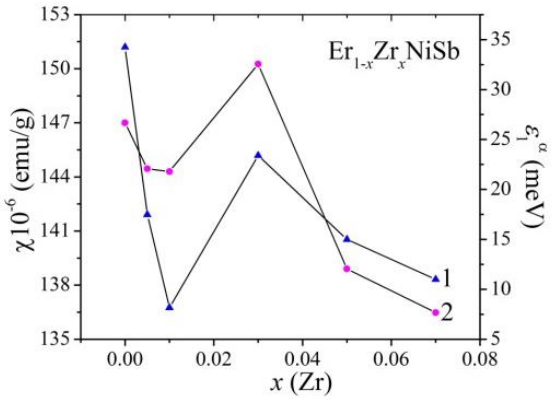

Fig. 5. Variation of the activation energy values $\varepsilon_1^{\alpha}(x)$ (1) and magnetic susceptibility $\chi(x)$ (2) at T = 300 K.

which is determined by free electrons and is proportional to the density of electronic states at Fermi level $g(\varepsilon_F)$. At concentrations $x > 0$, the dependence $\chi(x)$ decreases rapidly and passes through the minimum at x = 0.01. Subsequently, the $\chi(x)$ dependence grows, reaches a maximum at x = 0.03, and then decreases. Since the dependence $\chi(x)$ is proportional to $g(\varepsilon_F)$, the growth of $\chi(x)$ dependence for $Er_{1-x}Zr_xNiSb$ indicates an increase of the density of states at Fermi level $g(\varepsilon_F)$. The decrease of $\chi(x)$ dependence of $Er_{1-x}Zr_xNiSb$, at $x > 0.03$, indicates a decrease of the density of states at the Fermi level $g(\varepsilon_F)$, which can be caused by the metallization of electrical conductivity of the semiconductor.

The obtained and presented experimental results of the study of $Er_{1-x}Zr_xNiSb$ thermosensitive material are not enough for final conclusions concerning the atom distribution in the semiconductor and the construction of adequate models of electronic structure and mechanisms of electrical conductivity. This requires further research as a crystal structure, in particular, the possible existence of homogeneity range for ErNiSb compound, the study of $Er_{1-x}Zr_xNiSb$ at higher temperatures of homogenizing annealing, as well as electrokinetic and energetic characteristics combined with modeling of these characteristics, etc.

Conclusions

Thus, the presented above results indicate the complex nature of including of Zr atoms into the structure of the ErNiSb compound. It was suggested that the introduction of Zr atoms ($4d^25s^2$) into the structure of half-Heusler phase ErNiSb by substitution of Er ($5d^06s^2$) atoms in 4*a* position, the Zr atoms can also simultaneously occupy the 4*c* position of Ni atoms ($3d^84s^2$). As a result, in the $Er_{1-x}Zr_xNiSb$ semiconductor, both structural defects of donor nature in 4*a* position (Zr has a larger number of *d*-electrons than Er) and acceptor defects in the 4*c* position of Ni atoms (Ni has more 3*d*-electrons than Zr) are generated simultaneously. In this case, the energy states of impurity donor ε_D^2 and acceptor ε_A^1 bands (donor-acceptor pairs) appear which determine the mechanisms of electrical conduction of semiconductor.

Romaka V. **–** Proffesor;
Stadnyk Yu. **-** Ph.D., Senior Scientist;
Romaka L. **-** Ph.D., Senior Scientist;
Krayovskyy V. **-** Ph.D., associate professor;
Horyn A. **-** Ph.D., Senior Research;
Klyzub P. **–** student;
Pashkevych V. **-** docent.

[1] O. Sologub, P.S. Salamakha. Rare earth antimony: [in]: Gschneidner K. (Ed.), Handbook on the Physics and Chemistry of Rare Earths (The Netherlands, Amsterdam 2003).
[2] V.K. Pecharsky, J.V. Pankevich, O.I. Bodak, Sov. Phys. Crystallogr. (Ehgl. Transl) 28, 97 (1983).
[3] K. Harties, W. Jeitschko, J. Alloys Compd. 226, 81 (1995) (https://doi.org/10.1016/0925-8388(95)01573-6).
[4] V.A. Romaka, Yu.V. Stadnyk, V.Ya. Krayovskyy, L.P. Romaka, O.P. Guk, V.V. Romaka, M.M. Mykyichuk, A.M. Horyn, The nowel heat-sensitive materials and temperature transducers (Lviv Polytechnic Publishing House, Lviv, 2020).
[5] I. Karla, J. Pierre, R.V. Skolozdra, J. Alloys Compd. 265, 42 (1998) (https://doi.org/10.1016/S0925-8388(97)00419-2).
[6] V.A. Romaka, V.V. Romaka, Yu.V. Stadnyk, Intermetallic semiconductors: properties and applications (Lviv Polytechnic Publishing House, Lviv, 2011).
[7] Yu. Stadnyk, V.A. Romaka, A. Horyn, L. Romaka, V. Krayovskyy, I. Romaniv, M. Rokomanuk, Phys. Chem. Sol. St., 21(1), 73 (2020) (https://doi.org/10.15330/pcss.21.1.73-81).
[8] L.P. Romaka, D. Kaczorowski, A.M. Horyn, Yu.V. Stadnyk, V.Ya. Krayovskyy, V.V. Romaka, Phys. Chem. Solid State 17(1), 37 (2016) (https://doi.org/10.15330/pcss.17.1.37-42).
[9] T. Roisnel, J. Rodriguez-Carvajal, Mater. Sci. Forum, Proc. EPDIC7, 378-381, 118 (2001) (https://doi.org/10.4028/www.scientific.net/MSF.378-381.118).
[10] B.I. Shklovskii and A.L. Efros, Electronic Properties of Doped Semiconductors (Springer, NY, 1984).

В.А. Ромака[1], Ю. Стадник[2], Л. Ромака[2], В. Крайовський[1], А. Горинь[2], П. Клизуб[2], В. Пашкевич[1]

Дослідження структурних, кінетичних та магнітних характеристик напівпровідника $Er_{1-x}Zr_xNiSb$

[1]*Національний університет "Львівська політехніка, Львів, Україна, volodymyr.romaka@gmail.com*
[2]*Львівський національний університет ім. І.Франка, Львів, Україна, lyubov.romaka@gmail.com*

Досліджено особливості структурних, кінетичних, енергетичних та магнітних характеристик напівпровідникового твердого розчину $Er_{1-x}Zr_xNiSb$, x = 0 - 0.10. Зроблено припущення, що при уведенні атомів Zr ($4d^25s^2$) у структуру пів-Гейслерової фази ErNiSb шляхом заміщення у позиції 4*a* атомів Er ($5d^06s^2$) атоми Zr також одночасно можуть займати позицію 4*c* атомів Ni ($3d^84s^2$). Як результат, у напівпровіднику $Er_{1-x}Zr_xNiSb$ одночасно генеруються як структурні дефекти донорної природи у позиції 4*a* і акцепторної у позиції 4*c*. При цьому у забороненій зоні $Er_{1-x}Zr_xNiSb$ з'являються енергетичні стани домішкових донорної ε_D^2 та акцепторної ε_A^1 зон (донорно-акцепторні пари), які визначають механізми електропровідності напівпровідника.

Ключові слова: електропровідність, коефіцієнт термо-ерс, рівень Фермі.